HHS Public Access

Author manuscript

Nat Genet. Author manuscript; available in PMC 2011 April 01.

Published in final edited form as:

Nat Genet. 2010 July ; 42(7): 626–630. doi:10.1038/ng.593.

Lin28a transgenic mice manifest size and puberty phenotypes identified in human genetic association studies

Hao Zhu[1,3], **Samar Shah**[1,2], **Ng Shyh-Chang**[2], **Gen Shinoda**[2], **William S. Einhorn**[2,4], **Srinivas R. Viswanathan**[1,2], **Ayumu Takeuchi**[1,2], **Corinna Grasemann**[5,6], **John L. Rinn**[7,8], **Mary F. Lopez**[9], **Joel N. Hirschhorn**[7,9,11], **Mark R. Palmert**[5,6], and **George Q. Daley**[1,2,4,12,14,*]

[1]Stem Cell Transplantation Program, Division of Pediatric Hematology/Oncology, Children's Hospital Boston and Dana Farber Cancer Institute, Boston, Massachusetts, USA.

[2]Harvard Stem Cell Institute, Boston, Massachusetts, USA.

[3]Division of Medical Oncology, Dana Farber Cancer Institute, Boston, Massachusetts, USA.

[4]Division of Hematology, Brigham and Women's Hospital, Boston, Massachusetts, USA.

[5]Division of Endocrinology, The Hospital for Sick Children, Toronto, Canada.

[6]Department of Paediatrics, The University of Toronto, Canada.

[7]The Broad Institute of Harvard and Massachusetts Institute of Technology, Cambridge, Massachusetts, USA

[8]Department of Pathology, Beth Israel Deaconess Medical Center, Harvard Medical School, Boston, Massachusetts, USA

[9]Division of Endocrinology, Children's Hospital of Boston, Massachusetts, USA.

[10]Division of Genetics, Program in Genomics, Children's Hospital of Boston, Massachusetts, USA.

[11]Department of Genetics, Harvard Medical School, Boston, Massachusetts, USA.

*To Whom Correspondence should be Addressed: Phone:(617) 919-2013 Fax: (617) 730-0222 george.daley@childrens.harvard.edu.

Author Contributions H.Z. and G.Q.D. conceived experiments and wrote the manuscript. H.Z. performed all experiments unless otherwise indicated. S.S. contributed to the work in Figures 1, 2, 4 and Supplemental Figures S4 and S5. N.S.C. performed the GSEA microarray analysis and created Figures 4j-l. G.S. generated the data in Figures S1a and S1b. W.S.E. performed mouse husbandry, genotyping, and experiments in Figure S3d. S.R.V. made the *Lin28a* mouse ES cell line and mouse strain. A.T. performed the mouse chimera injections for the generation of all the transgenic strains. C.G. provided experimental assistance for puberty phenotyping and isolation/processing of endocrine organs. J.L.R., M.F.L., J.N.H. and M.R.P. contributed reagents, analyzed data, and edited the manuscript.

Database accession numbers

Listed below are the NCBI Reference Sequence numbers for the Lin28 family:

Mus musculus lin-28 homolog a (*C. elegans*) (*Lin28a*): NM_145833.1

Homo sapiens lin-28 homolog A (*C. elegans*) (*LIN28A*): NM_024674.4

Mus musculus lin-28 homolog B (*C. elegans*) (*Lin28b*): NM_001031772.1

Homo sapiens lin-28 homolog B (*C. elegans*) (*LIN28B*): NM_001004317.2

The data discussed in this publication have been deposited in NCBI's Gene Expression Omnibus and are accessible through GEO Series accession number GSE21226 (http://www.ncbi.nlm.nih.gov/geo/query/acc.cgi?acc=GSE21226).

[12]Department of Biological Chemistry and Molecular Pharmacology, Harvard Medical School, Boston, Massachusetts, USA.

[13]Howard Hughes Medical Institute, Boston, Massachusetts, USA.

[14]Manton Center for Orphan Disease Research, Boston, Massachusetts, USA.

Abstract

Recently, genome-wide association studies (GWAS) have linked the human *LIN28B* locus to height and timing of menarche [1-5]. LIN28B and its homolog LIN28 (hereafter, LIN28A) are functionally redundant RNA-binding proteins that block *let-7* microRNA (miRNA) biogenesis [6-9]. *lin-28* and *let-7* were discovered in *C. elegans* as heterochronic regulators of larval and vulval development, but recently have been implicated in cancer, stem cell aging, and pluripotency [10-13]. The *let-7* targets *Myc*, *Kras*, *Igf2bp1* and *Hmga2* are known regulators of mammalian body size and metabolism [14-18]. To explore the *Lin28/let-7* pathway *in vivo*, we engineered transgenic mice to express *Lin28a* and observed increased body size, crown-rump length, and a delayed onset of puberty. While investigating metabolic and endocrine mechanisms of overgrowth, we observed increased glucose metabolism and insulin sensitivity in these transgenic mice. We report a mouse that models the human phenotypes associated with genetic variation in the *Lin28/let-7* pathway.

To investigate *Lin28a* function *in vivo*, we generated a transgenic mouse strain that expresses the M2 reverse tetracycline transactivator (M2-rtTA) from the *Rosa26* locus and Flag-tagged mouse *Lin28a* from the *Collagen 1a1* (*Col1a1*) locus (Fig. 1a) [19]. We observed that mice carrying the *Lin28a* transgene (*Lin28a* Tg) were larger than non-transgenic littermates, even in the absence of the *rtTA* transgene and/or doxycycline induction. Transgene-bearing animals also had wider facies and coarser hair (Fig. 1b). *Lin28a* Tg animals showed an increased growth rate and in adulthood were heavier and longer (Fig. 1c-d). Newborn wild-type (WT) and *Lin28a* Tg pups were the same size (Fig. S1a). Differences in weight and crown-rump length became apparent after weaning, and the increased growth of Tg mice was characterized by a prolonged growth period with higher plateaus for height and weight. In contrast, we found that *Lin28a* knockout mice weigh 20% less at birth than WT pups, but do not survive long enough for further analysis (Fig. S1b).

DEXA imaging revealed no change in percentage body fat or lean mass in *Lin28a* Tg mice, but did show increased bone mineral content and density (Fig. 1e). Organ mass was increased in relative proportion to total body weight, suggesting appropriate regulation of organ size relative to overall body growth (Fig. 1f). To control for any possible effects of doxycycline induction of the engineered *Col1a1* locus, we generated a mouse strain using the KH2 embryonic stem cell (ESC) line without a targeted transgene. After 5 weeks of doxycycline, the WT, induced, and un-induced mice containing the engineered *Col1a1* allele showed no differences in weight (Fig. S1c). Taken together, our data show that *Lin28a* Tg mice possess increased body size, a phenotype associated with genetic variation in the human *LIN28B* locus.

Given the recent GWAS linking *LIN28B* to later age at menarche, we investigated the timing of reproductive maturity in these mice. Vaginal opening (VO) is a key milestone in sexual development and a reliable marker for the onset of murine puberty [20]. In *Lin28a* Tg mice, we observed a 2.24 and 2.18 day delay in VO in the CD-1 and C57BL/6J strains, respectively (Table 1 and Fig. 2a-b; both $p < 0.002$). Puberty was delayed despite the fact that *Lin28a* Tg mice were heavier at VO for both strain backgrounds (Table 1 and Fig. 2c; both $p < 0.0001$). At day 26 of age, uterine plus ovarian mass was greater in the WT mice, indicating delayed sexual development in Tg mice (Fig. 2d; $p < 0.002$). WT and *Lin28a* Tg mice achieved first estrus at day 27.3 and day 31.8, respectively (Fig. 2e; $p = 0.0106$). Furthermore, mating experiments revealed that *Lin28a* Tg animals had a ~3 day delay to date of first litter (Fig. 2f; $p = 0.0351$), correlating well with the delays in VO and first estrus. We noted that the size of the first litter was markedly larger in the Tg versus WT animals (16.4 vs. 9.67; $p = 0.0002$) (Fig. 2g), though overall fertility was no different over the first three months of life, indicating that altered timing of sexual maturation was not due to reproductive incompetence.

We then analyzed *Lin28a* transgene and *let-7* expression in various organs. Normally, both *Lin28a* and *Lin28b* are highly expressed in early murine embryogenesis until E10.5. Thereafter, their patterns diverge: *Lin28b* is expressed in the fetal liver, blood, and brain, while *Lin28a* is expressed in the intestinal crypts, muscle, heart, testes, and ovary [21]. By RT-PCR, combined transgene and endogenous *Lin28a* mRNA expression was increased in multiple organs in the Tg mice, resulting from ectopic expression of the *Lin28a* transgene from the *Col1A1* locus in both neonates and adults (Fig. 3a-b). In adults, there was a 7-fold *Lin28a* mRNA increase in the skeletal muscle, a 5-fold increase in the ovary, and a 4-fold increase in the hypothalamus (Fig. 3a). In the neonatal limb, which contains skin and muscle, there was a 3-fold increase (Fig. 3b). These fold changes were small, considering that endogenous *Lin28a* is expressed in these tissues. In the muscle, skin and neonatal limb, the additional *Lin28a* protein functioned to suppress *let-7* processing (Fig. 3c-d). In contrast, *let-7* levels were preserved in the liver, where *Lin28a* is absent (Fig. 3c-d). To corroborate these results, immunohistochemistry (IHC) was used to show increased Lin28a protein in skin and muscle (Fig 3e), but not in other tissues (Fig. S2). Within the hypothalamic-pituitary-gonadal axis (HPG axis), endogenous *Lin28a* is normally only expressed in the pituitary and ovary. Despite over-expression of *Lin28a* in the hypothalamus and ovary (Fig. 3a), we found no decrease of *let-7a* or *let-7g* in the HPG axis, demonstrating that *Lin28a* and *let-7* are uncoupled in some tissues(Fig. 3f).

In a separate study, we showed that doxycycline induction of *Lin28a* expression expands transit amplifying cell numbers in a cell autonomous manner in the intestinal crypts, blood, and skin (Viswanathan *et al.*, unpublished data), supporting the hypothesis that increased progenitor cell proliferation leads to organ and whole body enlargement. Doxycycline induction in *Lin28a* Tg animals leads to rapid death associated with marked gut pathology, thus precluding the analysis of growth phenotypes associated with higher levels of *Lin28a*. The un-induced Tg mice exhibited thickened skin, larger bones, and proportionally enlarged visceral organs. Microscopically, we noted hyperplasia of the skin and bone (Fig. 3g), but no differences in visceral organ histology (Fig. S2 and S3). Tg livers are 50-60% larger than

livers from WT littermates (Fig. 1f), and show increased proliferation as assayed by Ki-67, but no increase in cell size (Fig S3a-c). Skeletal muscle cell diameters were also the same (Fig. S3c). To determine if *Lin28a*, *LIN28B* or *let-7* could cause cell hypertrophy, we induced these genes in three doxycycline-inducible ESCs, and observed that cell size was unaffected (Fig. S3d). These data show that *Lin28a* mediates organ overgrowth by increasing cell numbers rather than cell size.

The proportional overgrowth suggested that endocrine or metabolic mechanisms might be governing organismal growth. We failed to observe pituitary adenomas and serum growth hormone and Igf1 were not elevated (Fig. S4), ruling out these etiologies of gigantism. Lin28a has been shown to enhance protein translation of Igf2, whose loss of imprinting causes a human overgrowth disorder called Beckwith-Wiedemann Syndrome (BWS) [22, 23]. We found a ~20-fold increase of *Igf2* mRNA in liver and a 2-fold increase in muscle (Fig. 4a). To determine if *Igf2* was driving overgrowth, we crossed *Lin28a* Tg females to *Igf2* null males and noted that *Lin28a* Tg mice lacking *Igf2* were still overgrown (Fig. S5a). We confirmed that *Igf2* coding mRNA was absent (Fig. S5b), ruling out an *Igf2* dependent mechanism.

BWS patients also exhibit hypoglycemia, leading us to test if enhanced glucose utilization was contributing to overgrowth [24]. We first found that fasting and fed glucose was lower in the Tg mice (Fig. 4b-c). Using the glucose tolerance test, we showed that both males and females cleared glucose more efficiently (Fig. 4d-e). Using the insulin tolerance test, we found that Tg mice also had increased insulin sensitivity (Fig. 4f-g). To show that the lower glucose was due to an increase in peripheral tissue sensitivity rather than an increase in secreted insulin, we showed that insulin levels at fasting and thirty minutes after a glucose challenge were both lower in Tg mice (Fig. 4h). Consistent with a chronically decreased need for insulin, islets were smaller in transgenic animals at two ages (Fig. 4i), further supporting the hypothesis that *Lin28a* mediates enhanced glucose uptake in peripheral tissues. Importantly, the *Lin28a* Tg mice lacking *Igf2* still showed enhanced glucose uptake and lower fed state glucose (Fig. S5c-d), demonstrating that this phenotype was not *Igf2* dependent.

Because *Lin28a* is normally expressed in muscle, a major organ for glucose processing, and because the Tg mice express 7-fold more *Lin28a* in muscle, we reasoned that over-expression in muscle might drive increased glucose uptake. We over-expressed *Lin28a* in C2C12 myoblasts, differentiated them for one week, and found increased 2-deoxy-D-[^{3}H] glucose (2-DG) uptake relative to controls (Fig. 4j). In contrast, shRNA knockdown of *Lin28a* in C2C12 led to a reduction in labeled glucose uptake (Fig. 4k), demonstrating that *Lin28a* is both necessary and sufficient for enhanced glucose uptake in these cells. To identify mechanisms involved in growth and glucose metabolism, we performed whole genome mRNA expression analysis in five week old skeletal muscle. Using gene-set enrichment analysis [25, 26], we found that expression signatures associated with *let-7* targets, hypoxia, and the *Ras* pathway were most significantly upregulated, while six of the fifteen most down-regulated sets involved oxidative phosphorylation or mitochondrial genes (Fig. 4). We hypothesized that increased glucose uptake, increased activity of hypoxia pathways and decreased oxidative phosphorylation represented an increase in glycolytic

metabolism. To test this, we measured serum lactate and found that *Lin28a* Tg mice generated more of this glycolytic metabolite than WT controls after glucose challenge (Fig. 4m). Together, these data suggest that over-expression of *Lin28a* in skeletal muscle alters the metabolic state of the tissue, driving enhanced glucose uptake and favoring glycolytic metabolism. As the M2 isoform of pyruvate kinase (PKM2) drives glycolysis in embryos and cancer cells [27, 28], we asked if *Lin28a* might be activating Pkm2 *in vivo*. However, no Pkm2 RNA or protein was detected in skeletal muscle or liver of adult WT or Tg animals, excluding Pkm2 expression as a mechanism for increased glycolysis in the *Lin28a* Tg mice (data not shown).

Because GWAS-identified polymorphisms are typically associated with modest changes in gene or *cis*-regulatory activity, it is difficult to ascertain whether SNPs are associated with gain or loss-of-function effects. In contrast, knockout or transgenic mice often demonstrate either dramatic phenotypes like lethality or no phenotype at all, making it difficult to model human genetic variation. When induced by doxycycline, the *Lin28a* Tg mice succumb to gene hyperfunction. In the un-induced state, phenotypes associated with variation at the human *LIN28B* locus and in the loci of *let-7* target genes were observed due to "leaky" expression that modestly alters *Lin28a* and *let-7* levels. Although Lin28a also has *let-7* independent functions, the fact that the *let-7* targets *DOTL1*, *HMGA2*, and *CDK6* are also associated with taller stature suggests that LIN28B acts through *let-7* to affect height [29]. Murine knockouts of many *let-7* targets such as *Hmga2*, *Igf2bp1*, and *Myc* are runted, suggesting that larger body size could result from reduced *let-7* suppression of its growth promoting targets [14-18]. In this mouse model, increased *Lin28a* in muscle results in a modest decrease of *let-7* and a global increase in *let-7* target gene expression (Fig. 4l). In *C. elegans*, loss of *lin-28* results in precocious vulval differentiation and premature developmental progression [30, 31], while loss of *let-7* leads to reiteration of larval stages and delayed differentiation [32]. We show that *Lin28a* gain of function also leads to a delay in murine puberty. Although increased body size and pre-pubescent growth rate are correlated with earlier menarche in humans [33], the *LIN28B* alleles associated with later menarche were also linked to taller stature [2-5]. Our model predicts that hyperfunction of LIN28B in humans contributes to increased height and later menarche, and indicate that some heterochronic functions of this pathway are conserved from worm to human.

In heterochronic fashion, Lin28a may also coordinate the rapid growth and metabolism of early embryogenesis and in turn delay the phenotypes associated with adulthood. We found that Lin28a causes increased glucose utilization, a mechanism by which it might drive overgrowth *in vivo*. *let-7* target oncogenes such as *MYC* and *KRAS* also have profound effects on metabolism [34, 35], as the anabolic demands of embryos or tumors must be met by a different type of metabolism. In cancer, this use of "aerobic glycolysis" is known as the Warburg Effect [36], a phenomenon that is just starting to be explored in embryonic development. The *Lin28a* Tg mouse represents an invaluable tool for sorting out the relationship between metabolism, growth, and developmental timing.

Methods

Generation of transgenic mice

Flag-tagged murine *Lin28a* open reading frame was cloned into pBS plasmid and targeting was performed into V6.5 ES cells containing *M2-rtTA* targeted to the *Rosa26* locus, as previously described [19]. Chimeric mice were generated by injection of ES cells into Balb/c blastocysts, then bred to CD-1 females to generate germline-transmitted pups. The line was maintained on the CD-1 background and the C57/B6 background by backcrossing 3-6 times. For all experiments, littermate controls were used.

Quantitative RT-PCR

RNA was collected by Trizol, reverse-transcribed using SuperScript II (Invitrogen). mRNA and miRNA expression was measured by quantitative PCR using the Delta-Delta CT method as described previously [10].

Histological Analysis

Tissue samples were fixed in 10% buffered formalin or Bouin's solution and embedded in paraffin. Immunostaining was performed by using the rabbit anti-Lin28a antibody from Proteintech group (used at 1:300; catalog number 11724-1-AP).

Immunohistochemistry

Sections of tissues were deparaffinized with xylene and rehydrated with graded series of ethanol (absolute, 95%, 80% and 50%, respectively, and distilled water), followed by two washes of 5 min each in PBS-T. Antigen retrieval was performed for 20 min in sodium citrate buffer (10mM pH 6) at 90-100°C followed by wash with PBST 1× 5 min. Tissue sections were then incubated for 10 min in 3% (v/v) hydrogen peroxide in methanol to block endogenous peroxidase activity. Sections were then washed for 5 min in PBS-T and blocked at room temperature for 1 h by using 2% normal goat serum, 2% bovine serum albumin (BSA) and 0.1% triton-X in PBS. Tissue sections were then incubated in humidified chamber for overnight incubation at 4°C with primary antibody (1/200 in TBST). Sections were subsequently washed with PBS-T (3× 5min) and incubated at room temperature for 1 h with secondary antibody (goat anti rabbit). After a wash with PBS-T (3× 5min), sections were incubated with ready to use streptavidin peroxidase (Lab Vision, Fremont, CA) for 10 min at room temperature and then color was developed by using a DAB kit (Vector laboratories, Burlingame, CA). Sections were counterstained with hematoxylin.

Glucose and insulin tolerance tests

Glucose tolerance tests were accomplished by intraperitoneal injection of glucose (2 g glucose/kg body weight) after an overnight fast (14–18h). Insulin tolerance was tested in 5 hour fasted mice by intraperitoneal injection of human regular insulin (0.75 U insulin/kg body weight; Lilly, Indianapolis, Indiana). Blood glucose was determined with a One Touch Basic glucometer (Lifescan, Milipitas, California). Insulin, GH, and Igf1 levels were measured by enzyme-linked immunosorbent assays (Crystal Chem, Chicago, Illinois).

Cloning and Plasmid Construction

Murine *Lin28a* cDNA was subcloned into pBabe.Puro and pMSCV.Neo retroviral vectors. *Lin28a* shRNA in lentiviral plasmid was purchased from Sigma-Aldrich (TRCN0000122599). Control shRNA was commercially purchased (SHC002V, Sigma-Aldrich)

Viral Production

For ecotropic viral production, retroviral plasmid DNA and pCL-Eco were transfected into 293T cells in a 1:1 mass ratio and virus harvested after 48h. For VSV-G pseudotyped lentivirus, viral plasmid, lentiviral gag/pol, and VSV-G were transfected in a mass ratio 1:0.9:0.1, and virus was harvested after 72 hrs. 1 mL of unconcentrated viral supernatant was used to infect 50,000 cells. Infected cells were selected on antibiotic prior to subsequent analysis.

Glucose uptake assay

C2C12 cells growth, differentiation, and glucose uptake was performed as described in Berti et al [37].

Puberty phenotyping analysis

Beginning on the day of weaning, female pups were examined daily, 7 d/wk, between 0800 and 1300 h, and the age at VO and concurrent body weight were recorded [38, 39]. For uteri/ovary weights, females were sacked at day 26 after birth and organs were weighed. For mating, a male proven to be fertile was placed into a cage with two WT or two Tg females at 21 days of age and the first litter date and size were recorded. Estrus analysis was performed as describe previously [40].

Statistical analysis

Data is presented as mean ± SEM, and Student's t-test (two-tailed distribution, two-sample unequal variance) was used to calculate P values. Statistical significance is displayed as $p < 0.05$ (one asterisk) or $p < 0.01$ (two asterisks).

Microarray

RNA from quadriceps muscle from 5 week old WT and Tg mice (n = 2 and 2) were harvested and processed using RNeasy mini kits from Qiagen. All RNA samples were DNase treated. The Illumina Ref-8 microarray platform was used to generate data.

Gene set analysis

Gene Set Enrichment Analysis was used to identify gene sets/pathways associated with a set of upregulated or downregulated genes. Gene Set Enrichment Analysis 9 (version 2.0) is an analytic tool for relating gene expression data to gene sets to identify unifying biological themes [25, 26].

Supplementary Material

Refer to Web version on PubMed Central for supplementary material.

Acknowledgements

We would like to acknowledge John Powers, Harith Rajagopalan and Michael Kharas for invaluable discussions and advice regarding this work. We would also like to thank Yuin-Han Loh, Morris White, Lulu Wang and Joseph Majzoub for in-depth discussion and endocrine expertise.

REFERENCES

1. Lettre G, et al. Identification of ten loci associated with height highlights new biological pathways in human growth. Nat Genet. 2008; 40(5):584–91. [PubMed: 18391950]
2. Ong KK, et al. Genetic variation in LIN28B is associated with the timing of puberty. Nat Genet. 2009
3. Sulem P, et al. Genome-wide association study identifies sequence variants on 6q21 associated with age at menarche. Nat Genet. 2009
4. He C, et al. Nat Genet. 2009
5. Perry JR, et al. Meta-analysis of genome-wide association data identifies two loci influencing age at menarche. Nat Genet. 2009
6. Viswanathan SR, Daley GQ, Gregory RI. Selective blockade of microRNA processing by Lin28. Science. 2008; 320(5872):97–100. [PubMed: 18292307]
7. Newman MA, Thomson JM, Hammond SM. Lin-28 interaction with the Let-7 precursor loop mediates regulated microRNA processing. RNA. 2008:1539–49. [PubMed: 18566191]
8. Chang TC, et al. Lin-28B transactivation is necessary for Myc-mediated let-7 repression and proliferation. Proc Natl Acad Sci U S A. 2009; 106(9):3384–9. [PubMed: 19211792]
9. Dangi-Garimella S, et al. Raf kinase inhibitory protein suppresses a metastasis signalling cascade involving LIN28 and let-7. EMBO J. 2009; 28(4):347–58. [PubMed: 19153603]
10. Viswanathan SR, et al. Lin28 promotes transformation and is associated with advanced human malignancies. Nat Genet. 2009; 41(7):843–8. [PubMed: 19483683]
11. Nishino J, et al. Hmga2 Promotes Neural Stem Cell Self-Renewal in Young but Not Old Mice by Reducing p16Ink4a and p19Arf Expression. Cell. 2008:227–239. [PubMed: 18957199]
12. Yu F, et al. let-7 regulates self renewal and tumorigenicity of breast cancer cells. Cell. 2007; 131(6):1109–23. [PubMed: 18083101]
13. Yu J, et al. Induced pluripotent stem cell lines derived from human somatic cells. Science. 2007; 318(5858):1917–20. [PubMed: 18029452]
14. Trumpp A, et al. c-Myc regulates mammalian body size by controlling cell number but not cell size. Nature. 2001:768–73. [PubMed: 11742404]
15. Weedon MN, et al. A common variant of HMGA2 is associated with adult and childhood height in the general population. Nat Genet. 2007; 39(10):1245–50. [PubMed: 17767157]
16. Christiansen J, et al. IGF2 mRNA-binding protein 2: biological function and putative role in type 2 diabetes. J Mol Endocrinol. 2009; 43(5):187–95. [PubMed: 19429674]
17. Hansen TV, et al. Dwarfism and impaired gut development in insulin-like growth factor II mRNA-binding protein 1-deficient mice. Mol Cell Biol. 2004; 24(10):4448–64. [PubMed: 15121863]
18. Zhou X, et al. Mutation responsible for the mouse pygmy phenotype in the developmentally regulated factor HMGI-C. Nature. 1995; 376(6543):771–4. [PubMed: 7651535]
19. Hochedlinger K, et al. Ectopic expression of Oct-4 blocks progenitor-cell differentiation and causes dysplasia in epithelial tissues. Cell. 2005; 121(3):465–77. [PubMed: 15882627]
20. Krewson TD, et al. Chromosomes 6 and 13 harbor genes that regulate pubertal timing in mouse chromosome substitution strains. Endocrinology. 2004; 145(10):4447–51. [PubMed: 15284200]
21. Yang DH, Moss EG. Temporally regulated expression of Lin-28 in diverse tissues of the developing mouse. Gene Expr Patterns. 2003:719–26. [PubMed: 14643679]

22. Polesskaya A, et al. Lin-28 binds IGF-2 mRNA and participates in skeletal myogenesis by increasing translation efficiency. Genes & Development. 2007:1125–38. [PubMed: 17473174]
23. Sun FL, et al. Transactivation of Igf2 in a mouse model of Beckwith-Wiedemann syndrome. Nature. 1997; 389(6653):809–15. [PubMed: 9349812]
24. Elliott M, et al. Clinical features and natural history of Beckwith-Wiedemann syndrome: presentation of 74 new cases. Clin Genet. 1994; 46(2):168–74. [PubMed: 7820926]
25. Subramanian A, et al. Gene set enrichment analysis: a knowledge-based approach for interpreting genome-wide expression profiles. Proc Natl Acad Sci U S A. 2005; 102(43):15545–50. [PubMed: 16199517]
26. Mootha VK, et al. PGC-1alpha-responsive genes involved in oxidative phosphorylation are coordinately downregulated in human diabetes. Nat Genet. 2003; 34(3):267–73. [PubMed: 12808457]
27. Christofk HR, et al. The M2 splice isoform of pyruvate kinase is important for cancer metabolism and tumour growth. Nature. 2008; 452(7184):230–3. [PubMed: 18337823]
28. Clower CV, et al. The alternative splicing repressors hnRNP A1/A2 and PTB influence pyruvate kinase isoform expression and cell metabolism. Proc Natl Acad Sci U S A. 107(5):1894–9. [PubMed: 20133837]
29. Lettre G, et al. Identification of ten loci associated with height highlights new biological pathways in human growth. Nat Genet. 2008:584–91. [PubMed: 18391950]
30. Moss EG, Lee RC, Ambros V. The cold shock domain protein LIN-28 controls developmental timing in C. elegans and is regulated by the lin-4 RNA. Cell. 1997; 88(5):637–46. [PubMed: 9054503]
31. Nimmo RA, Slack FJ. An elegant miRror: microRNAs in stem cells, developmental timing and cancer. Chromosoma. 2009; 118(4):405–18. [PubMed: 19340450]
32. Abbott AL, et al. The let-7 MicroRNA family members mir-48, mir-84, and mir-241 function together to regulate developmental timing in Caenorhabditis elegans. Dev Cell. 2005; 9(3):403–14. [PubMed: 16139228]
33. Biro FM, et al. Impact of timing of pubertal maturation on growth in black and white female adolescents: The National Heart, Lung, and Blood Institute Growth and Health Study. J Pediatr. 2001; 138(5):636–43. [PubMed: 11343036]
34. Yun J, et al. Glucose deprivation contributes to the development of KRAS pathway mutations in tumor cells. Science. 2009; 325(5947):1555–9. [PubMed: 19661383]
35. Gao P, et al. c-Myc suppression of miR-23a/b enhances mitochondrial glutaminase expression and glutamine metabolism. Nature. 2009; 458(7239):762–5. [PubMed: 19219026]
36. Vander Heiden MG, Cantley LC, Thompson CB. Understanding the Warburg effect: the metabolic requirements of cell proliferation. Science. 2009; 324(5930):1029–33. [PubMed: 19460998]
37. Berti L, Gammeltoft S. Leptin stimulates glucose uptake in C2C12 muscle cells by activation of ERK2. Mol Cell Endocrinol. 1999; 157(1-2):121–30. [PubMed: 10619403]
38. Nathan BM, Hodges CA, Palmert MR. The use of mouse chromosome substitution strains to investigate the genetic regulation of pubertal timing. Mol Cell Endocrinol. 2006; 254-255:103–8. [PubMed: 16762493]
39. Nathan BM, et al. A Quantitative Trait Locus on Chromosome 6 Regulates the Onset of Puberty in Mice. Endocrinology. 2006:5132–5138. [PubMed: 16873534]
40. Mettus RV, Rane SG. Characterization of the abnormal pancreatic development, reduced growth and infertility in Cdk4 mutant mice. Oncogene. 2003; 22(52):8413–21. [PubMed: 14627982]

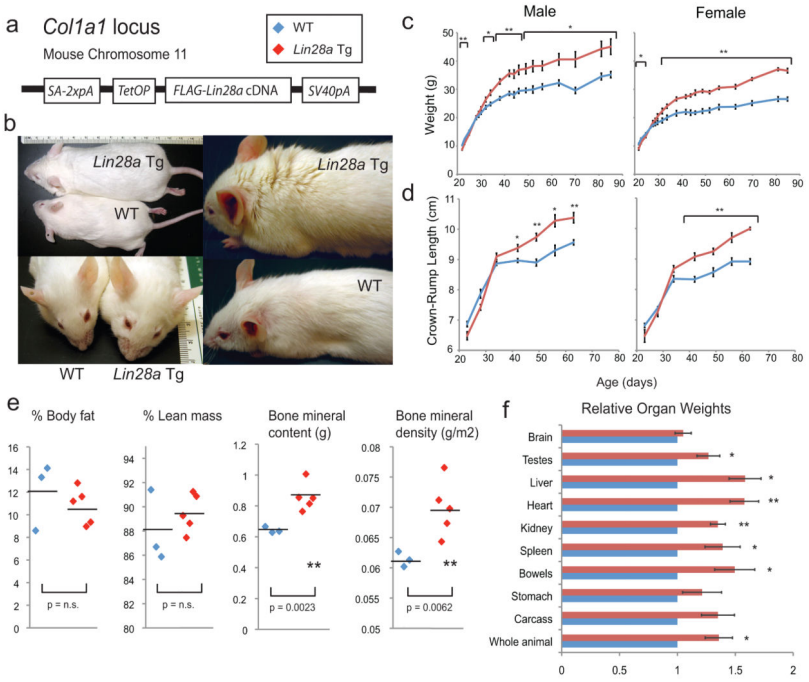

Figure 1. *Lin28a* inducible mice display increased growth and a proportional increase in organ sizes

(a) Schema for the design of the *Lin28a* transgenic mice. Animals under study were not induced with doxycycline. (b) Adult *Lin28a* Tg mice exhibited greater size, wider facies, larger ears, and coarser hair than WT mice. (c-d) Male (4 WT and 5 Tg) and female (6 WT and 4 Tg) weights and crown-rump lengths from weaning until three months of age. (e) Dual Energy X-ray Absorptiometry results showing percent body fat mass, percent lean mass, bone mineral content, and bone mineral density (g/bone area (m^2)) for 3 WT and 5 Tg males. (f) Relative organ weights of Tg animals normalized to WT animals (n = 7 and 7). All values represent means +/− SEM (*, $p < 0.05$; **, $p < 0.01$) and the numbers of mice (n) are shown in the chart or noted in the legend.

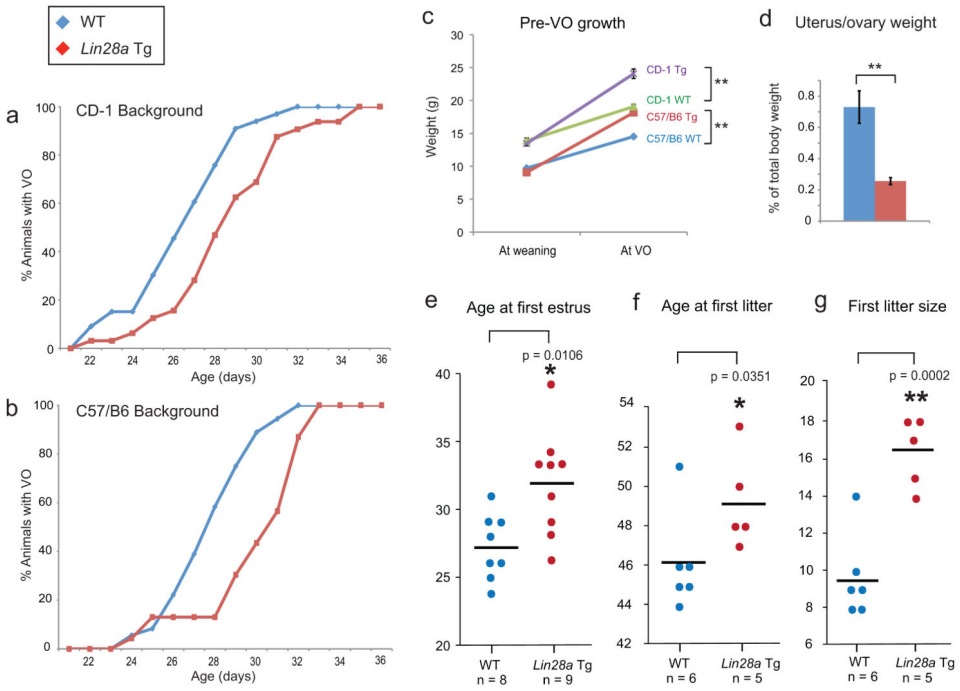

Figure 2. *Lin28a* Tg mice show a delay in the onset of puberty

(a-b) Comparison of the timing of vaginal opening (VO) in WT (blue) and transgenic mice (red) on the CD-1 (a) and C57/B6 backgrounds (b). The cumulative percent of animals with VO is displayed. (c) Weights of WT and *Lin28a* Tg mice at date of weaning and time of VO. (d) Uterus/ovary weights measured as a percentage of total body weight at day 26 of age (n = 10 and 8). (e) The time to first estrus. (f) The time to first litter. (g) The first litter size from these matings. All values represent means +/− SEM (*, $p < 0.05$; **, $p < 0.01$) and the numbers of mice (n) are shown in the chart or noted in the legend.

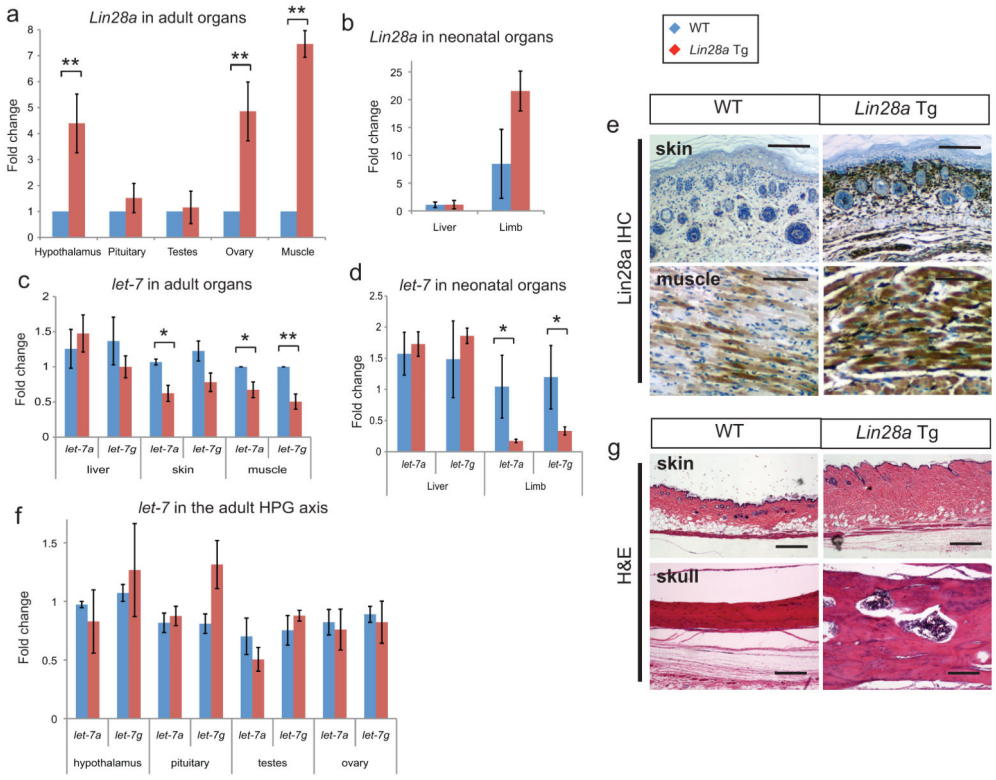

Figure 3. Ectopic expression of *Lin28a* in transgenic mice

Lin28a mRNA levels in adult (a) and neonatal organs (b) as measured by quantitative PCR (n = 6 and 6 for all analyses). (c-d) Mature *let-7a* and *let-7g* levels in the adult liver, skin, and muscle (c) and in the liver and limb of neonates (d). (e) Lin28a immunohistochemistry in neonatal skin and muscle. (f) *let-7a* and *let-7g* in the hypothalamic-pituitary-gonadal axis of adult mice. (g) Histology of skin and skull bone in 4 month-old WT and Tg adults. All scale bars are 100μm. All values represent means +/− SEM (*, $p < 0.05$; **, $p < 0.01$) and the numbers of mice (n) are noted here.

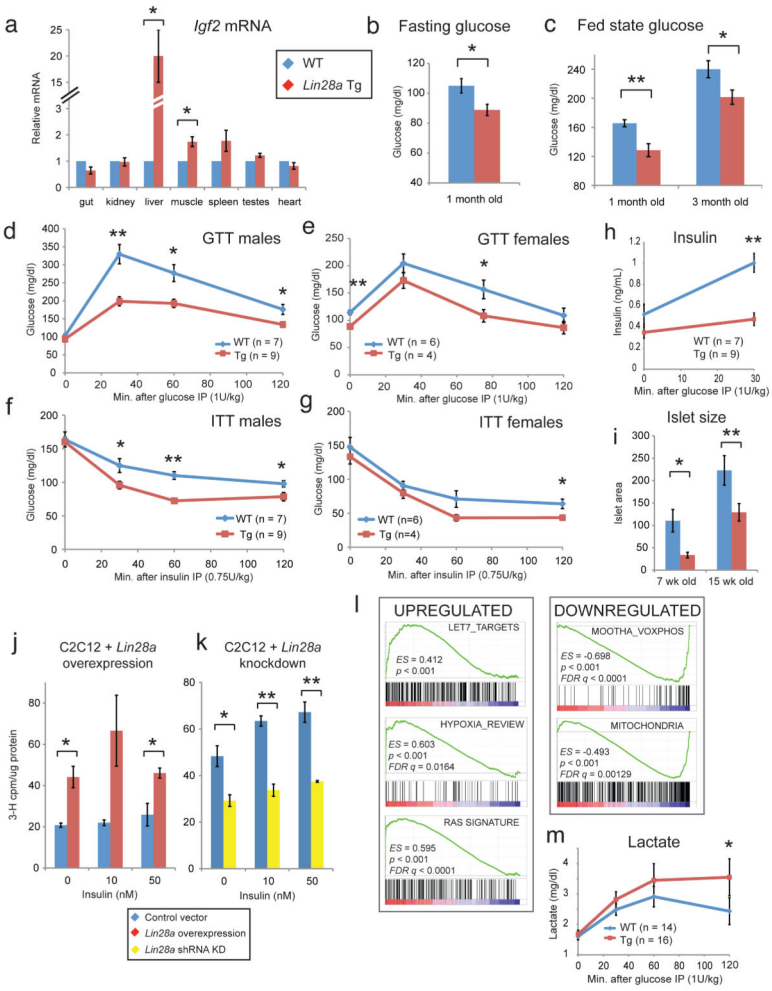

Figure 4. *Lin28a* Tg mice display increased glucose uptake and insulin sensitivity

(a) *Igf2* mRNA levels in adult mouse tissues. Note the break in the *y*-axis designating a change in scale. (b-c) Glucose concentrations in fasting and fed state mice. Blood glucose and insulin concentrations were determined by tail bleeding in 1 or 3 month-old mice. Experimental groups consisted of 5-10 animals each. (d-e) Results of glucose tolerance tests (GTT) and (f-g) insulin tolerance tests (ITT) for WT and *Lin28a* Tg mice. GTT and ITT were performed on 1-3 month-old mice with 0.75 units of insulin/kg of body weight and 2 g of glucose/kg of body weight, respectively. (h) Insulin measurements performed during a GTT. (i) Average islet area measurements in 7 week old (n = 2 and 2) or 15 week old pancreata (n = 3 and 3) (8 to 40 islet analyzed per animal). (j-k) 2-deoxy-D-[^{3}H] glucose uptake assay with C2C12 + *Lin28a* overexpression (j) and C2C12 + *Lin28a* shRNA knockdown (k). (l) Gene set enrichment analysis of muscle microarray data showing statistically significantly up and downregulated pathways in Tg vs. WT skeletal muscle. (m) Lactate levels were measured using Lactate Scout strips during a GTT experiment. All values represent means +/− SEM (*, $p < 0.05$; **, $p < 0.01$) and the numbers of experimental animals are listed within the charts.

Table 1

Mean age and body weight at time of VO are increased in *Lin28a* Tg mice.

Strain	Mean age (days) at VO (mean +/− SD)	N	P vs WT (VO)	Body weight (g) at VO (mean +/− SD)
CD-1 WT	26.64 +/− 2.5	33		19.08 +/− 1.9
CD-1 *Lin28a* Tg	28.88 +/− 2.8	32	0.00146	24.00 +/− 4.3
C57/B6 WT	28.08 +/− 2.0	36		14.60 +/− 1.1
C57/B6 *Lin28a* Tg	30.26 +/− 2.6	23	0.00144	18.17 +/− 2.0